

CERN-EP-2017-237
11 September 2017

J/ψ elliptic flow in Pb–Pb collisions at $\sqrt{s_{NN}} = 5.02$ TeV

ALICE Collaboration*

Abstract

We report a precise measurement of the J/ψ elliptic flow in Pb–Pb collisions at $\sqrt{s_{NN}} = 5.02$ TeV with the ALICE detector at the LHC. The J/ψ mesons are reconstructed at mid-rapidity ($|y| < 0.9$) in the dielectron decay channel and at forward rapidity ($2.5 < y < 4.0$) in the dimuon channel, both down to zero transverse momentum. At forward rapidity, the elliptic flow v_2 of the J/ψ is studied as a function of transverse momentum and centrality. A positive v_2 is observed in the transverse momentum range $2 < p_T < 8$ GeV/ c in the three centrality classes studied and confirms with higher statistics our earlier results at $\sqrt{s_{NN}} = 2.76$ TeV in semi-central collisions. At mid-rapidity, the J/ψ v_2 is investigated as a function of transverse momentum in semi-central collisions and found to be in agreement with the measurements at forward rapidity. These results are compared to transport model calculations. The comparison supports the idea that at low p_T the elliptic flow of the J/ψ originates from the thermalization of charm quarks in the deconfined medium, but suggests that additional mechanisms might be missing in the models.

arXiv:1709.05260v1 [nucl-ex] 15 Sep 2017

© 2017 CERN for the benefit of the ALICE Collaboration.

Reproduction of this article or parts of it is allowed as specified in the CC-BY-4.0 license.

*See Appendix A for the list of collaboration members

Extreme conditions of temperature and pressure created in ultra-relativistic heavy-ion collisions enable exploration of the phase diagram region where Quantum Chromodynamics (QCD) predicts the existence of a deconfined state, the Quark-Gluon Plasma (QGP) [1, 2]. Heavy quarks are produced through hard-scattering processes prior to the formation of the QGP and experience the evolution through interactions in the medium. Therefore, the measurement of bound states of heavy quarks is expected to provide sensitive probes of the strongly-interacting medium [3]. Among the quarkonium resonances, the J/ψ meson has been extensively studied in nucleus-nucleus collisions. Theoretical calculations based on lattice QCD predict a J/ψ suppression to be induced by the screening of the color force in a deconfined medium which becomes stronger as the temperature increases [4, 5]. In a complementary way to this static approach, J/ψ suppression can be seen also as the result of dynamical interactions with the surrounding partons [6–8]. Within these scenarios, the suppression of the J/ψ, experimentally quantified via the nuclear modification factor R_{AA} , is expected to increase with the initial temperature (energy density) of the QGP, hence with the collision energy. However, the suppression of inclusive J/ψ with transverse momentum $p_{\text{T}} < 8$ GeV/c observed by the ALICE Collaboration in Pb–Pb collisions at $\sqrt{s_{\text{NN}}} = 2.76$ TeV [9] is smaller than that at lower energies at the Super Proton Synchrotron (SPS) [10] and Relativistic Heavy Ion Collider (RHIC) [11–14] and exhibits almost no centrality dependence. Furthermore, in central collisions the suppression decreases from high to low transverse momentum [15, 16]. Recently the ALICE Collaboration reported the inclusive ¹ J/ψ R_{AA} down to zero transverse momentum at forward rapidity ($2.5 < y < 4$) in Pb–Pb collisions at $\sqrt{s_{\text{NN}}} = 5.02$ TeV [17]. The results at $\sqrt{s_{\text{NN}}} = 5.02$ TeV are compatible with the previous measurements at $\sqrt{s_{\text{NN}}} = 2.76$ TeV. The J/ψ R_{AA} enhancement from RHIC to LHC energies can be explained by theoretical models [6–8, 18–20] that include a dominant contribution from J/ψ (re)generation through (re)combination of thermalized charm quarks in the medium, during or at the phase boundary of the deconfined phase ².

Additional observables, like the azimuthal anisotropy of particle production, are required to better constrain theoretical models and study the interplay between the J/ψ suppression and regeneration mechanisms [21]. Studies of collective phenomena have greatly contributed to the characterization of the system created in heavy-ion collisions [22]. The anisotropy of the final-state particle momentum distribution has been found to be sensitive to the geometry and the dynamics of the early stages of the collisions. The spatial anisotropy in the initial matter distribution due to the nuclear overlap region in non-central collisions is transferred to the final momentum distribution via multiple collisions in a strongly coupled system [23]. The beam axis and the impact parameter vector of the colliding nuclei define the reaction plane. The second coefficient of the Fourier expansion v_2 describes the final state particle azimuthal distribution with respect to the reaction plane and is called elliptic flow.

Within the transport model scenario [7, 20], the observed J/ψ have two origins. First, primordial and decay J/ψ produced in the initial hard scatterings traverse and interact with the medium. During this process they may dissociate. Second, J/ψ can be (re)generated from deconfined charm quarks in the QGP. Because of the elliptic shape of the fireball, primordial J/ψ emitted along the short axis of the ellipsoid (in-plane) traverse a shorter path through the medium than those emitted along the longer axis (out-of-plane). However, transport models predict that this effect results in a small azimuthal anisotropy for the surviving J/ψ. In contrast, (re)generated J/ψ inherit the flow of the (re)combined charm quarks. If charm quarks do thermalize in the QGP, then J/ψ can exhibit a large elliptic flow. The regeneration component is expected to dominate at low p_{T} ($p_{\text{T}} \lesssim 6$ GeV/c) and the primordial J/ψ component to take over at higher p_{T} .

At RHIC, the STAR Collaboration measured, in Au–Au collisions at $\sqrt{s_{\text{NN}}} = 200$ GeV, a J/ψ v_2 consis-

¹Inclusive J/ψ include prompt J/ψ (direct and decays from higher mass charmonium states) and non-prompt J/ψ (feed down from b-hadron decays). In this Letter, all J/ψ measurements refer to inclusive J/ψ production unless otherwise stated.

²The terms (re)generation and (re)combination denote the two possible mechanisms of generation of J/ψ by combination of charm quarks at the QGP phase boundary and the continuous dissociation and recombination of charm quarks during the QGP evolution.

tent with zero, albeit with large uncertainties [24]. At the LHC a first indication of positive J/ψ v_2 was observed by the ALICE Collaboration in semi-central Pb–Pb collisions at $\sqrt{s_{\text{NN}}} = 2.76$ TeV with a 2.7σ significance for inclusive J/ψ with $2 < p_{\text{T}} < 6$ GeV/ c and $2.5 < y < 4.0$ [25]. The CMS Collaboration also reported a positive v_2 for prompt J/ψ at high p_{T} and mid-rapidity [26]. A precision measurement of the J/ψ elliptic flow in Pb–Pb collisions at the highest LHC energy will provide valuable insights on the J/ψ production mechanisms and on the thermalization of charm quarks. Indeed, at $\sqrt{s_{\text{NN}}} = 5.02$ TeV, the higher energy density of the medium should favor the charm quark thermalization, and thus increase its flow. In addition, the larger number of produced $c\bar{c}$ pairs should favor the formation of J/ψ by regeneration mechanisms, both leading to an increase of the observed J/ψ v_2 .

In this Letter, we report ALICE results on inclusive J/ψ elliptic flow in Pb–Pb collisions at $\sqrt{s_{\text{NN}}} = 5.02$ TeV in two rapidity ranges. At forward rapidity ($2.5 < y < 4.0$) the J/ψ are measured via the $\mu^+\mu^-$ decay channel and at mid-rapidity ($|y| < 0.9$) via the e^+e^- decay channel. The results are presented as a function of transverse momentum. For the dimuon channel different collision centralities are also investigated.

The ALICE detector is described in [27]. At forward rapidity ($2.5 < y < 4$) the production of quarkonia is measured with the muon spectrometer³ down to $p_{\text{T}} = 0$. The spectrometer consists of a front absorber stopping the hadrons followed by five tracking stations comprising two planes of cathode pad chambers each, with the third station inside a dipole magnet. The tracking apparatus is completed by a triggering system made of four planes of resistive plate chambers downstream of an iron wall, which absorbs secondary hadrons escaping from the front absorber and low momentum muons.

The central barrel detectors are used for the measurement of the quarkonium production at mid-rapidity ($|y| < 0.9$) down to $p_{\text{T}} = 0$ [28]. Charged particle tracking is performed by the Inner Tracking System (ITS) [29] and the Time Projection Chamber (TPC) [30], with the six layers of the ITS covering the radial range from the beam axis of 3.9 cm to 43.0 cm and the TPC from 85 to 247 cm. Both detectors cover $|\eta| < 0.9$ and the full azimuth. The specific ionization energy loss (dE/dx) in the gas of the TPC is used for particle identification (PID). In addition the Silicon Pixel Detector (SPD) is used to determine the location of the interaction point. The SPD corresponds to the two innermost layers of the ITS covering $|\eta| < 2.0$ and $|\eta| < 1.4$ for the inner and outer layer, respectively. The V0 counters [31], consisting of two arrays of 32 scintillator sectors each distributed in four rings covering $2.8 \leq \eta \leq 5.1$ (V0-A) and $-3.7 \leq \eta \leq -1.7$ (V0-C), are used as trigger and centrality detectors. As described later, the SPD, TPC, V0-A, and V0-C are also used as event plane detectors. All of these detectors have full azimuthal coverage.

The data were collected in 2015. The analysis at mid-rapidity uses minimum bias (MB) Pb–Pb collisions. The MB trigger requires a signal in both V0-A and V0-C and is fully efficient for the centrality range 0–90%. At forward rapidity, the analysis uses opposite-sign dimuon (MU) triggered Pb–Pb collisions. The MU trigger requires a MB trigger and at least a pair of opposite-sign track segments in the muon trigger system, each with a p_{T} above the threshold of the on-line trigger algorithm. This p_{T} threshold was set to provide 50% efficiency for muon tracks with $p_{\text{T}} = 1$ GeV/ c . The beam-induced background was further reduced offline using the V0 and the zero degree calorimeter (ZDC) timing information. The contribution from electromagnetic processes was removed by requiring a minimum energy deposited in the neutron ZDCs [32]. The centrality determination is based on a Glauber fit of the total V0 signal amplitude distribution as described in [33, 34]. The resulting data samples correspond to integrated luminosities of $\mathcal{L}_{\text{int}} \approx 13 \mu\text{b}^{-1}$ and $\mathcal{L}_{\text{int}} \approx 225 \mu\text{b}^{-1}$ at mid- and forward rapidity, respectively.

J/ψ candidates at forward- or mid-rapidity are formed by combining pairs of opposite-sign tracks reconstructed in the geometrical acceptance of the muon spectrometer or central barrel, respectively. The

³In the ALICE reference frame, the muon spectrometer covers a negative η range and consequently a negative y range. We have chosen to present our results with a positive y notation, due to the symmetry of the collision system.

reconstructed tracks in the muon tracking chambers at forward rapidity are required to match a track segment in the muon trigger system above the aforementioned p_T threshold. At mid-rapidity the reconstructed tracks must pass an electron selection criterion based on the expected dE/dx for electrons in the TPC [30].

The dimuon v_2 is calculated using event plane (EP) based methods. The angle of the reaction plane of the collision is estimated, event by event, by the second harmonic event plane angle Ψ [35], which is obtained from the azimuthal distribution of reconstructed tracks in the TPC or track segments in the SPD for the mid- and forward rapidity analyses, respectively. Effects of non-uniform acceptance in the determination of the EP are corrected using the methods described in [36]. At mid-rapidity, in order to remove auto-correlations the EP was calculated for each electron pair subtracting the contribution of the tracks forming the pair. The elliptic flow was determined as $v_2 = \langle \cos 2(\phi - \Psi) \rangle$, ϕ being the azimuthal angle of the reconstructed dilepton pair.

The J/ψ v_2 results were obtained, as proposed in [37], by fitting the distribution of the v_2 versus the invariant mass ($m_{\ell\ell}$) of the opposite-sign dilepton pairs. The total flow $v_2(m_{\ell\ell})$ is the combination of the signal and the background flow and can be expressed as

$$v_2(m_{\ell\ell}) = v_2^{\text{sig}} \alpha(m_{\ell\ell}) + v_2^{\text{bkg}}(m_{\ell\ell})[1 - \alpha(m_{\ell\ell})], \quad (1)$$

where v_2^{sig} and v_2^{bkg} correspond to the elliptic flow of the J/ψ signal (S) and of the background (B), respectively (see bottom panels of Fig. 1). The signal fraction $\alpha(m_{\ell\ell}) = S(m_{\ell\ell}) / (S(m_{\ell\ell}) + B(m_{\ell\ell}))$ was extracted from fits to the invariant mass distribution (see top panels of Fig. 1) in each p_T and centrality class.

At forward rapidity, the J/ψ peak (S-term of $\alpha(m_{\ell\ell})$) is fit either with an extended Crystal Ball function or a pseudo-Gaussian with a mass-dependent width [38]. The underlying continuum (B-term of $\alpha(m_{\ell\ell})$) is described with the ratio of second- to third-order polynomials, a pseudo-Gaussian with a width quadratically varying with mass, or Chebyshev polynomials of order six. The background flow v_2^{bkg} was parametrized using a second-order polynomial, a Chebyshev polynomial of order four, or the product of a first order polynomial and an exponential function. At mid rapidity, the underlying continuum was estimated combining opposite-sign electrons from different events (using an event-mixing technique) or combining same-sign electrons from the same event. After removing the underlying continuum, the J/ψ signal was obtained by counting the number of dielectron pairs or from a fit with a MC-generated shape. The background flow was parametrized using a second-, third- or fifth-order polynomial depending on the p_T class. Additionally, the PID and track-quality selection criteria were varied as part of the systematic uncertainty evaluation.

The J/ψ v_2 and its statistical uncertainty in each p_T and centrality class were determined as the average of the v_2^{sig} obtained by fitting $v_2(m_{\ell\ell})$ using Eq. 1 with the various $\alpha(m_{\ell\ell})$ and $v_2^{\text{bkg}}(m_{\ell\ell})$ parametrizations in several invariant mass ranges, while the corresponding systematic uncertainties were defined as the RMS of these results. Figure 1 shows typical fits of the opposite-sign dimuon invariant mass distribution (top) and of $\langle \cos 2(\phi - \Psi) \rangle$ as a function of $m_{\ell\ell}$ (bottom) at forward (left) and mid (right) rapidity in the 20–40% centrality class. A similar method was used to extract the uncorrected (for detector acceptance and efficiency) average transverse momentum $\langle p_T \rangle^{\text{uncor}}$ of the reconstructed J/ψ in each centrality and p_T class. The $\langle p_T \rangle^{\text{uncor}}$ is used to locate the data points when plotted as a function of p_T . Consistent v_2 values were obtained using an alternative method [35] in which the J/ψ raw yield is extracted, as described before, in bins of $(\phi - \Psi)$ and v_2 is evaluated by fitting the data with the function $\frac{dN}{d(\phi - \Psi)} = A[1 + 2v_2 \cos 2(\phi - \Psi)]$, where A is a normalization constant.

A correlation of J/ψ mesons with the particles used to determine the event plane could also originate from other sources, commonly denoted non-flow, which are not related to the correlation with the initial geometry symmetry plane, such as higher-mass particle decays or jets. Their effect was estimated to be

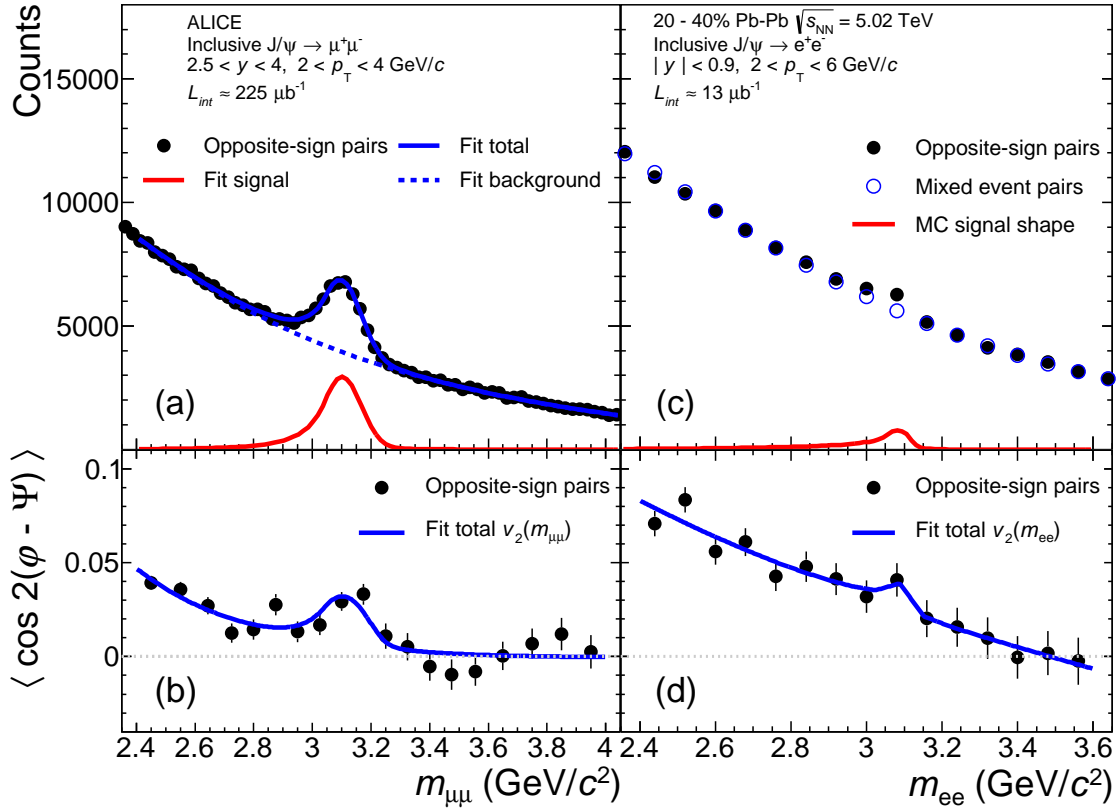


Fig. 1: (color online) Invariant mass distribution (top) and $\langle \cos 2(\varphi - \Psi) \rangle$ as a function of $m_{\ell\ell}$ (bottom) of opposite-sign dimuons (left) with $2 < p_T < 4$ GeV/c and $2.5 < y < 4$ and dielectrons (right) with $2 < p_T < 6$ GeV/c and $|y| < 0.9$, in semi-central (20–40%) Pb-Pb collisions.

small with respect to the other uncertainties by repeating the analysis at forward rapidity using the event plane determined in either V0-A ($\Delta\eta = 5.3$) or V0-C (no η gap) detector.

The finite resolution in the EP determination smears out the azimuthal distributions and lowers the value of the measured anisotropy [35]. The SPD- and TPC-based resolutions as a function of the centrality were determined by applying the 3 sub-event method [35] which consists in comparing the event plane angles obtained with different sub-groups of particles, on a sample of MB events. For the SPD (TPC), the 3 sub-events were obtained using V0-A, V0-C and SPD, with $\Delta\eta_{V0A-SPD}=1.4$ ($\Delta\eta_{V0A-TPC}=1.9$), $\Delta\eta_{V0A-V0C}=4.5$ and $\Delta\eta_{SPD-V0C}=0.3$ ($\Delta\eta_{TPC-V0C}=0.8$) pseudo-rapidity gaps. The contribution to the systematic uncertainty from the EP determination was estimated exploiting the availability of different sub-events, built from the multiplicity measurement in the V0-A or V0-C, track segments in the SPD, and tracks in the TPC. The related uncertainty is estimated to be 1% and is assigned to the EP resolution. Since v_2 is measured here in a wide centrality class, the related resolution must reflect the distribution of events with a J/ψ for each centrality class. Therefore, the EP resolution for each wide class was calculated as the average of the values obtained in finer centrality classes weighted by the number of reconstructed J/ψ . Table 1 shows the corresponding resolution for each centrality class, which is applied to the forward rapidity results reported in this Letter. For the mid-rapidity result, the TPC EP resolution is 0.880 ± 0.009 (syst) in the centrality class 20–40%.

At forward rapidity, the J/ψ reconstruction efficiency depends on the detector occupancy, which could bias the v_2 measurement. This effect was evaluated by embedding azimuthally isotropic simulated $J/\psi \rightarrow \mu^+\mu^-$ decays into real events. The measured v_2 of the embedded J/ψ does not deviate from zero by more than 0.006 in the centrality and p_T classes considered. This value is used as a conservative systematic

Centrality	$\langle N_{part} \rangle$	EP resolution
5–20%	287 ± 4	0.873 ± 0.009
20–40%	160 ± 3	0.910 ± 0.009
40–60%	70 ± 2	0.832 ± 0.008

Table 1: Average number of participants $\langle N_{part} \rangle$ and SPD EP resolution for each centrality class (expressed in percentage of the nuclear cross section) [34]. The quoted uncertainties are systematic.

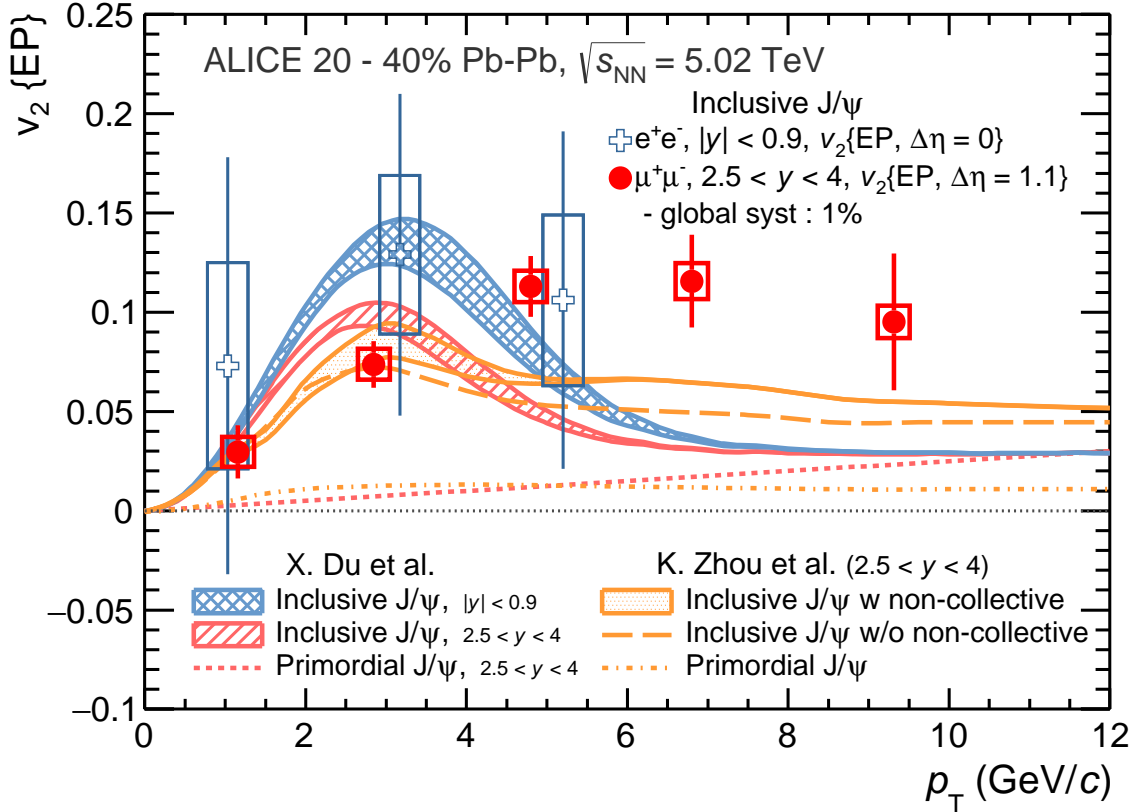


Fig. 2: (color online) Inclusive J/ψ $v_2(p_T)$ at forward and mid-rapidity for semi-central (20–40%) Pb–Pb collisions at $\sqrt{s_{NN}} = 5.02$ TeV (see text for details on uncertainties). Calculations from transports model by [39] and [8] are also shown (see text for details).

uncertainty on all measured v_2 values.

Figure 2 shows J/ψ $v_2(p_T)$ at forward and mid-rapidity in semi-central (20–40%) Pb–Pb collisions at $\sqrt{s_{NN}} = 5.02$ TeV. The p_T ranges are 0–2, 2–4, 4–6, 6–8, and 8–12 GeV/c and 0–2, 2–6, and 4–12 GeV/c at forward and mid-rapidity, respectively. The vertical bars indicate the statistical uncertainties, while the boxes indicate the point-to-point uncorrelated systematic uncertainties. The global relative systematic uncertainty on the EP resolution is 1.0% and is correlated with p_T . At forward rapidity, a non-zero v_2 is observed in the measured p_T range for semi-central collisions (20–40%). Including statistical and systematic uncertainties the significance of a non-zero v_2 is as large as 6.6σ in the p_T class 4–6 GeV/c. The observed J/ψ v_2 increases with transverse momentum up to $v_2 = 0.113 \pm 0.015(\text{stat}) \pm 0.008(\text{syst})$ at $4 < p_T < 6$ GeV/c. The J/ψ $v_2(p_T)$ at mid-rapidity is similar to that at forward rapidity, albeit with large uncertainties. At mid-rapidity, the J/ψ v_2 in the range $2 < p_T < 6$ GeV/c is $v_2 = 0.129 \pm 0.080(\text{stat}) \pm 0.040(\text{syst})$.

Transport model calculations that include a large J/ψ (re)generation component from deconfined charm

quarks in the medium [8, 39, 40] are also shown in Fig. 2. In the model by Du *et al.* [39] (TM1) the v_2 of inclusive J/ψ (hashed red band at forward rapidity and double-hashed blue band at mid-rapidity) has three origins. First, thermalized charm quarks in the medium transfer a significant elliptic flow to (re)generated J/ψ. Second, primordial J/ψ traverse a longer path through the medium when emitted out-of-plane than in-plane resulting in a small apparent v_2 . Third, if b quarks do thermalize then their elliptic flow will be transferred to b-hadrons at hadronization and to non-prompt J/ψ from the b-hadron decay. The second component (survival probability of primordial J/ψ) is represented as a dashed red line to highlight the small J/ψ v_2 in the absence of heavy-quark collective flow. The model by Zhou *et al.* [8] (TM2), in addition to the previous components, also includes a non-collective J/ψ v_2 component. This latter component arises from the modification of the quarkonium production in the presence of a strong magnetic field in the early stage of the heavy-ion collision [41]. In Fig. 2 the calculations of the TM2 are shown at forward rapidity with (shaded orange band) and without (long-dashed orange line) the non-collective J/ψ v_2 component. As for TM1, the v_2 resulting from the different in-plane than out-of-plane survival probability of primordial J/ψ is shown as a dash-dotted orange line.

TM1 [39] is able to describe qualitatively the J/ψ nuclear modification factor measurements by ALICE reported in [17]. The model also agrees within uncertainties with ALICE J/ψ v_2 measurement at forward rapidity at $\sqrt{s_{\text{NN}}} = 2.76$ TeV [25] and at mid-rapidity at $\sqrt{s_{\text{NN}}} = 5.02$ TeV. However, at high p_{T} ($p_{\text{T}} > 4$ GeV/c), clear discrepancies are observed between the model and the J/ψ v_2 at forward rapidity and $\sqrt{s_{\text{NN}}} = 5.02$ TeV. It is worth noting that some tension is also seen between the calculations of this model and the nuclear modification factor measurement by ALICE in this higher p_{T} range in [17]. At low p_{T} ($p_{\text{T}} \leq 4$ GeV/c), the model reproduces the magnitude of the measurement by a dominant contribution of J/ψ elliptic flow inherited from thermalized charm quarks. However, the overall shape of the $v_2(p_{\text{T}})$ is missed and the results at high p_{T} are underestimated by the model. This disagreement suggests a missing mechanism in the model. Similar conclusions can be derived from the comparison of the forward rapidity data to TM2 [8] in the absence of the non-collective v_2 component [41]. The addition of the v_2 arising from a possible strong magnetic field in the early stage of heavy ion collisions improves the comparison with the measured J/ψ v_2 at forward rapidity, especially at high p_{T} . Such non-collective component was able to reproduce the prompt J/ψ v_2 at high p_{T} measured by CMS in Pb–Pb collisions at $\sqrt{s_{\text{NN}}} = 2.76$ TeV [26].

Figure 3 presents the p_{T} dependence of the J/ψ v_2 at forward rapidity for three centrality classes, 5–20%, 20–40%, and 40–60%. As in semi-central (20–40%) collisions, a significant v_2 is also observed for J/ψ with $2 < p_{\text{T}} < 8$ GeV/c in the 5–20% and 40–60% centrality classes. The transverse momentum dependence of the J/ψ v_2 at forward rapidity is consistent within uncertainties in the three centrality classes presented here. The J/ψ $v_2(p_{\text{T}})$ appears to be maximum for the 20–40% centrality class and tends to decrease for more central or peripheral collisions. It is interesting to note that for identified light hadrons in Pb–Pb collisions at $\sqrt{s_{\text{NN}}} = 2.76$ TeV, the $v_2(p_{\text{T}})$ is maximum in the 40–60% centrality class and decreases for more central collisions [42]. This different behavior can be understood in the framework of transport models by the increasing contribution of J/ψ regeneration for more central collisions [39, 40].

Also shown in Fig. 3 is the $v_2(p_{\text{T}})$ of prompt D-mesons in Pb–Pb collisions at $\sqrt{s_{\text{NN}}} = 5.02$ TeV for the 30–50% centrality class measured by ALICE at mid-rapidity [43]. The vertical bars indicate the statistical uncertainties, the open boxes the point-to-point uncorrelated systematic uncertainties and the shaded boxes the feed-down uncertainties. Although the centrality and rapidity ranges are different, it is clear that at low p_{T} ($p_{\text{T}} < 4$ GeV/c) the v_2 of D mesons is higher than that of J/ψ mesons. This feature supports the (re)generation for J/ψ mesons and thus the conclusion that both D and J/ψ mesons inherit their elliptic flow from thermalized charm quarks.

In summary, we report the ALICE measurements of inclusive J/ψ elliptic flow at forward and mid-rapidity in Pb–Pb collisions at $\sqrt{s_{\text{NN}}} = 5.02$ TeV. At forward rapidity, the transverse momentum dependence of the J/ψ v_2 was measured in the 5–20%, 20–40%, and 40–60% centrality classes for $p_{\text{T}} < 12$

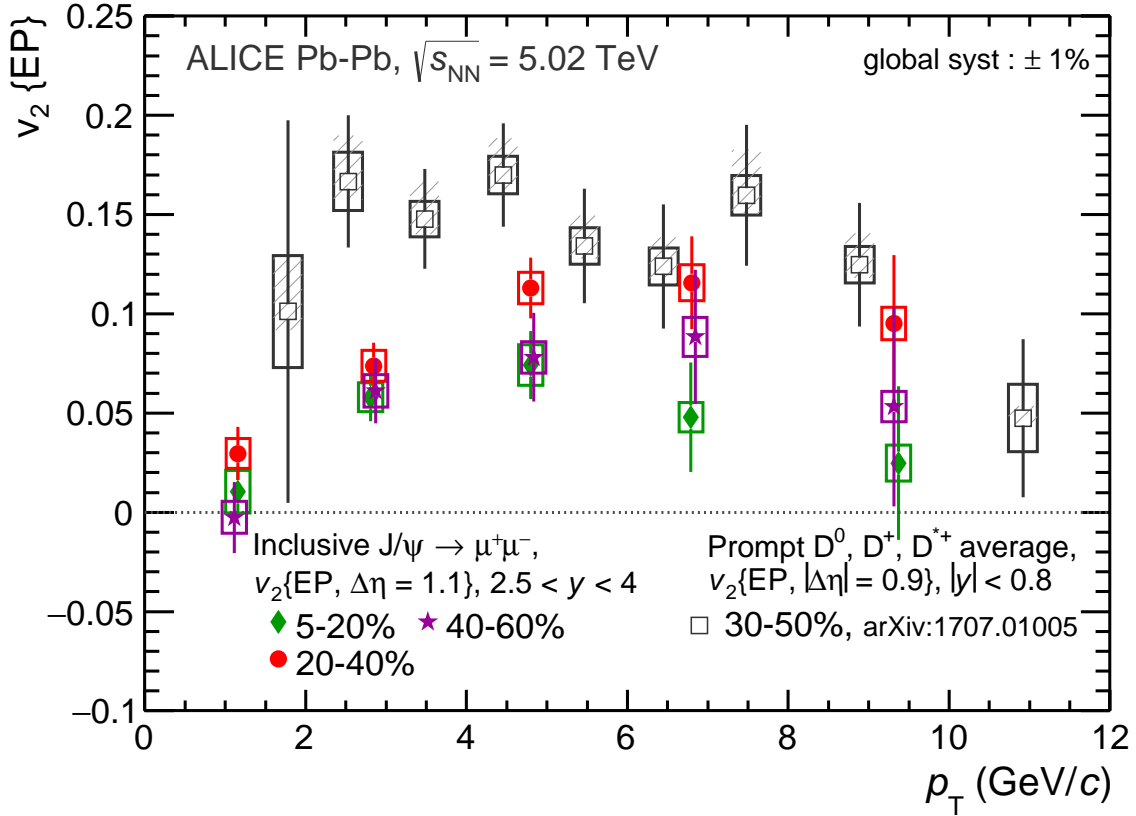


Fig. 3: (color online) Inclusive J/ψ $v_2(p_T)$ at forward rapidity in Pb–Pb collisions at $\sqrt{s_{NN}} = 5.02$ TeV for three centrality classes, 5–20%, 20–40%, and 40–60%. The average of D^0 , D^+ and D^{*+} $v_2(p_T)$ at mid- y in the centrality class 30–50% is also shown for comparison [43].

GeV/c. For all the reported centrality classes a significant J/ψ v_2 signal is observed in the intermediate region $2 < p_T < 8$ GeV/c. The results unambiguously establish for the first time that J/ψ mesons exhibit collective flow. At mid-rapidity, the transverse momentum dependence of the J/ψ v_2 was measured in semi-central 20–40% collisions and is found to be similar to the measurement at forward rapidity, albeit with larger uncertainties. The ALICE measurements of the J/ψ azimuthal anisotropy and nuclear modification factor impose strong constraints on theoretical models. At high p_T , transport models underestimate the measured J/ψ v_2 and (to a lesser extent) the R_{AA} . The origin of such discrepancy is currently not understood and suggests a missing mechanism in the models. At low p_T , the magnitude of the observed v_2 is achieved within transport models implementing a strong J/ψ (re)generation component from (re)combination of thermalized charm quarks in the QGP. Thus, the measurement of the J/ψ elliptic flow combined with the R_{AA} provides substantial evidence for thermalized charm quarks and (re)generation of J/ψ .

Acknowledgements

The ALICE Collaboration would like to thank all its engineers and technicians for their invaluable contributions to the construction of the experiment and the CERN accelerator teams for the outstanding performance of the LHC complex. The ALICE Collaboration gratefully acknowledges the resources and support provided by all Grid centres and the Worldwide LHC Computing Grid (WLCG) collaboration. The ALICE Collaboration acknowledges the following funding agencies for their support in building and running the ALICE detector: A. I. Alikhanyan National Science Laboratory (Yerevan Physics Institute) Foundation (ANSL), State Committee of Science and World Federation of Scientists (WFS), Armenia; Austrian Academy of Sciences and Nationalstiftung für Forschung, Technologie und Entwick-

lung, Austria; Ministry of Communications and High Technologies, National Nuclear Research Center, Azerbaijan; Conselho Nacional de Desenvolvimento Científico e Tecnológico (CNPq), Universidade Federal do Rio Grande do Sul (UFRGS), Financiadora de Estudos e Projetos (Finep) and Fundação de Amparo à Pesquisa do Estado de São Paulo (FAPESP), Brazil; Ministry of Science & Technology of China (MSTC), National Natural Science Foundation of China (NSFC) and Ministry of Education of China (MOEC), China; Ministry of Science, Education and Sport and Croatian Science Foundation, Croatia; Ministry of Education, Youth and Sports of the Czech Republic, Czech Republic; The Danish Council for Independent Research — Natural Sciences, the Carlsberg Foundation and Danish National Research Foundation (DNRF), Denmark; Helsinki Institute of Physics (HIP), Finland; Commissariat à l’Energie Atomique (CEA) and Institut National de Physique Nucléaire et de Physique des Particules (IN2P3) and Centre National de la Recherche Scientifique (CNRS), France; Bundesministerium für Bildung, Wissenschaft, Forschung und Technologie (BMBF) and GSI Helmholtzzentrum für Schwerionenforschung GmbH, Germany; General Secretariat for Research and Technology, Ministry of Education, Research and Religions, Greece; National Research, Development and Innovation Office, Hungary; Department of Atomic Energy Government of India (DAE), Department of Science and Technology, Government of India (DST), University Grants Commission, Government of India (UGC) and Council of Scientific and Industrial Research (CSIR), India; Indonesian Institute of Science, Indonesia; Centro Fermi - Museo Storico della Fisica e Centro Studi e Ricerche Enrico Fermi and Istituto Nazionale di Fisica Nucleare (INFN), Italy; Institute for Innovative Science and Technology, Nagasaki Institute of Applied Science (IIST), Japan Society for the Promotion of Science (JSPS) KAKENHI and Japanese Ministry of Education, Culture, Sports, Science and Technology (MEXT), Japan; Consejo Nacional de Ciencia (CONACYT) y Tecnología, through Fondo de Cooperación Internacional en Ciencia y Tecnología (FONCICYT) and Dirección General de Asuntos del Personal Académico (DGAPA), Mexico; Nederlandse Organisatie voor Wetenschappelijk Onderzoek (NWO), Netherlands; The Research Council of Norway, Norway; Commission on Science and Technology for Sustainable Development in the South (COMSATS), Pakistan; Pontificia Universidad Católica del Perú, Peru; Ministry of Science and Higher Education and National Science Centre, Poland; Korea Institute of Science and Technology Information and National Research Foundation of Korea (NRF), Republic of Korea; Ministry of Education and Scientific Research, Institute of Atomic Physics and Romanian National Agency for Science, Technology and Innovation, Romania; Joint Institute for Nuclear Research (JINR), Ministry of Education and Science of the Russian Federation and National Research Centre Kurchatov Institute, Russia; Ministry of Education, Science, Research and Sport of the Slovak Republic, Slovakia; National Research Foundation of South Africa, South Africa; Centro de Aplicaciones Tecnológicas y Desarrollo Nuclear (CEADEN), Cubaenergía, Cuba, Ministerio de Ciencia e Innovación and Centro de Investigaciones Energéticas, Medioambientales y Tecnológicas (CIEMAT), Spain; Swedish Research Council (VR) and Knut & Alice Wallenberg Foundation (KAW), Sweden; European Organization for Nuclear Research, Switzerland; National Science and Technology Development Agency (NSDTA), Suranaree University of Technology (SUT) and Office of the Higher Education Commission under NRU project of Thailand, Thailand; Turkish Atomic Energy Agency (TAEK), Turkey; National Academy of Sciences of Ukraine, Ukraine; Science and Technology Facilities Council (STFC), United Kingdom; National Science Foundation of the United States of America (NSF) and United States Department of Energy, Office of Nuclear Physics (DOE NP), United States of America.

References

- [1] J. D. Bjorken, “Highly Relativistic Nucleus-Nucleus Collisions: The Central Rapidity Region,” *Phys. Rev.* **D27** (1983) 140–151.
- [2] Y. Aoki, G. Endrodi, Z. Fodor, S. D. Katz, and K. K. Szabo, “The Order of the quantum chromodynamics transition predicted by the standard model of particle physics,” *Nature* **443** (2006) 675–678, arXiv:hep-lat/0611014 [hep-lat].

- [3] A. Andronic *et al.*, “Heavy-flavour and quarkonium production in the LHC era: from proton–proton to heavy-ion collisions,” *Eur. Phys. J.* **C76** no. 3, (2016) 107, arXiv:1506.03981 [nucl-ex].
- [4] T. Matsui and H. Satz, “J/ψ Suppression by Quark-Gluon Plasma Formation,” *Phys. Lett.* **B178** (1986) 416–422.
- [5] S. Digal, P. Petreczky, and H. Satz, “Quarkonium feed down and sequential suppression,” *Phys. Rev.* **D64** (2001) 094015, arXiv:hep-ph/0106017 [hep-ph].
- [6] E. G. Ferreira, “Charmonium dissociation and recombination at LHC: Revisiting comovers,” *Phys. Lett.* **B731** (2014) 57–63, arXiv:1210.3209 [hep-ph].
- [7] X. Zhao and R. Rapp, “Medium Modifications and Production of Charmonia at LHC,” *Nucl. Phys.* **A859** (2011) 114–125, arXiv:1102.2194 [hep-ph].
- [8] K. Zhou, N. Xu, Z. Xu, and P. Zhuang, “Medium effects on charmonium production at ultrarelativistic energies available at the CERN Large Hadron Collider,” *Phys. Rev.* **C89** no. 5, (2014) 054911, arXiv:1401.5845 [nucl-th].
- [9] ALICE Collaboration, B. Abelev *et al.*, “J/ψ suppression at forward rapidity in Pb-Pb collisions at $\sqrt{s_{NN}} = 2.76$ TeV,” *Phys. Rev. Lett.* **109** (2012) 072301, arXiv:1202.1383 [hep-ex].
- [10] NA50 Collaboration, B. Alessandro *et al.*, “A New measurement of J/ψ suppression in Pb-Pb collisions at 158-GeV per nucleon,” *Eur. Phys. J.* **C39** (2005) 335–345, arXiv:hep-ex/0412036 [hep-ex].
- [11] PHENIX Collaboration, A. Adare *et al.*, “J/ψ Production vs Centrality, Transverse Momentum, and Rapidity in Au+Au Collisions at $\sqrt{s_{NN}} = 200$ GeV,” *Phys. Rev. Lett.* **98** (2007) 232301, arXiv:nucl-ex/0611020 [nucl-ex].
- [12] PHENIX Collaboration, A. Adare *et al.*, “J/ψ suppression at forward rapidity in Au+Au collisions at $\sqrt{s_{NN}} = 200$ GeV,” *Phys. Rev.* **C84** (2011) 054912, arXiv:1103.6269 [nucl-ex].
- [13] STAR Collaboration, L. Adamczyk *et al.*, “J/ψ production at low p_T in Au+Au and Cu+Cu collisions at $\sqrt{s_{NN}} = 200$ GeV with the STAR detector,” *Phys. Rev.* **C90** no. 2, (2014) 024906, arXiv:1310.3563 [nucl-ex].
- [14] STAR Collaboration, L. Adamczyk *et al.*, “Energy dependence of J/ψ production in Au+Au collisions at $\sqrt{s_{NN}} = 39, 62.4$ and 200 GeV,” *Phys. Lett.* **B771** (2017) 13–20, arXiv:1607.07517 [hep-ex].
- [15] ALICE Collaboration, J. Adam *et al.*, “Differential studies of inclusive J/ψ and ψ(2S) production at forward rapidity in Pb-Pb collisions at $\sqrt{s_{NN}} = 2.76$ TeV,” *JHEP* **05** (2016) 179, arXiv:1506.08804 [nucl-ex].
- [16] ALICE Collaboration, B. B. Abelev *et al.*, “Centrality, rapidity and transverse momentum dependence of J/ψ suppression in Pb-Pb collisions at $\sqrt{s_{NN}}=2.76$ TeV,” *Phys. Lett.* **B734** (2014) 314–327, arXiv:1311.0214 [nucl-ex].
- [17] ALICE Collaboration, J. Adam *et al.*, “J/ψ suppression at forward rapidity in Pb-Pb collisions at $\sqrt{s_{NN}} = 5.02$ TeV,” *Phys. Lett.* **B766** (2017) 212–224, arXiv:1606.08197 [nucl-ex].
- [18] P. Braun-Munzinger and J. Stachel, “(Non)thermal aspects of charmonium production and a new look at J / psi suppression,” *Phys. Lett.* **B490** (2000) 196–202, arXiv:nucl-th/0007059 [nucl-th].

- [19] A. Andronic, P. Braun-Munzinger, K. Redlich, and J. Stachel, “The thermal model on the verge of the ultimate test: particle production in Pb–Pb collisions at the LHC,” *J. Phys.* **G38** (2011) 124081, arXiv:1106.6321 [nucl-th].
- [20] Y.-p. Liu, Z. Qu, N. Xu, and P.-f. Zhuang, “J/ψ Transverse Momentum Distribution in High Energy Nuclear Collisions at RHIC,” *Phys. Lett.* **B678** (2009) 72–76, arXiv:0901.2757 [nucl-th].
- [21] Y. Liu, N. Xu, and P. Zhuang, “J/ψ elliptic flow in relativistic heavy ion collisions,” *Nucl. Phys.* **A834** (2010) 317C–319C, arXiv:0910.0959 [nucl-th]. and Priv. Comm.
- [22] S. A. Voloshin, A. M. Poskanzer, and R. Snellings, “Collective phenomena in non-central nuclear collisions,” arXiv:0809.2949 [nucl-ex].
- [23] J.-Y. Ollitrault, “Anisotropy as a signature of transverse collective flow,” *Phys. Rev.* **D46** (1992) 229–245.
- [24] STAR Collaboration, L. Adamczyk *et al.*, “Measurement of J/ψ Azimuthal Anisotropy in Au+Au Collisions at $\sqrt{s_{NN}} = 200$ GeV,” *Phys. Rev. Lett.* **111** (2013) 052301, arXiv:1212.3304 [nucl-ex].
- [25] ALICE Collaboration, E. Abbas *et al.*, “J/ψ Elliptic Flow in Pb–Pb Collisions at $\sqrt{s_{NN}} = 2.76$ TeV,” *Phys. Rev. Lett.* **111** (2013) 162301, arXiv:1303.5880 [nucl-ex].
- [26] CMS Collaboration, V. Khachatryan *et al.*, “Suppression and azimuthal anisotropy of prompt and nonprompt J/ψ production in PbPb collisions at $\sqrt{s_{NN}} = 2.76$ TeV,” *Eur. Phys. J.* **C77** no. 4, (2017) 252, arXiv:1610.00613 [nucl-ex].
- [27] ALICE Collaboration, K. Aamodt *et al.*, “The ALICE experiment at the CERN LHC,” *JINST* **3** (2008) S08002.
- [28] ALICE Collaboration, B. Abelev *et al.*, “Inclusive J/ψ production in pp collisions at $\sqrt{s} = 2.76$ TeV,” *Phys. Lett.* **B718** (2012) 295–306, arXiv:1203.3641 [hep-ex]. [Erratum: *Phys. Lett.* B748,472(2015)].
- [29] ALICE Collaboration, K. Aamodt *et al.*, “Alignment of the ALICE Inner Tracking System with cosmic-ray tracks,” *JINST* **5** (2010) P03003, arXiv:1001.0502 [physics.ins-det].
- [30] J. Alme *et al.*, “The ALICE TPC, a large 3-dimensional tracking device with fast readout for ultra-high multiplicity events,” *Nucl. Instrum. Meth.* **A622** (2010) 316–367, arXiv:1001.1950 [physics.ins-det].
- [31] ALICE Collaboration, E. Abbas *et al.*, “Performance of the ALICE VZERO system,” *JINST* **8** (2013) P10016, arXiv:1306.3130 [nucl-ex].
- [32] ALICE Collaboration, B. Abelev *et al.*, “Measurement of the Cross Section for Electromagnetic Dissociation with Neutron Emission in Pb–Pb Collisions at $\sqrt{s_{NN}} = 2.76$ TeV,” *Phys. Rev. Lett.* **109** (2012) 252302, arXiv:1203.2436 [nucl-ex].
- [33] ALICE Collaboration, B. Abelev *et al.*, “Centrality determination of Pb–Pb collisions at $\sqrt{s_{NN}} = 2.76$ TeV with ALICE,” *Phys. Rev.* **C88** no. 4, (2013) 044909, arXiv:1301.4361 [nucl-ex].
- [34] ALICE Collaboration, J. Adam *et al.*, “Centrality dependence of the charged-particle multiplicity density at midrapidity in Pb–Pb collisions at $\sqrt{s_{NN}} = 5.02$ TeV,” *Phys. Rev. Lett.* **116** no. 22, (2016) 222302, arXiv:1512.06104 [nucl-ex].

- [35] A. M. Poskanzer and S. Voloshin, “Methods for analyzing anisotropic flow in relativistic nuclear collisions,” *Phys. Rev.* **C58** (1998) 1671–1678, arXiv:nucl-ex/9805001 [nucl-ex].
- [36] I. Selyuzhenkov and S. Voloshin, “Effects of non-uniform acceptance in anisotropic flow measurement,” *Phys. Rev.* **C77** (2008) 034904, arXiv:0707.4672 [nucl-th].
- [37] N. Borghini and J. Ollitrault, “Azimuthally sensitive correlations in nucleus-nucleus collisions,” *Phys. Rev.* **C70** (2004) 064905, arXiv:nucl-th/0407041 [nucl-th].
- [38] ALICE Collaboration, “Quarkonium signal extraction in ALICE,” *ALICE-PUBLIC-2015-006* (Oct, 2015) . <https://cds.cern.ch/record/2060096>.
- [39] X. Du and R. Rapp, “Sequential Regeneration of Charmonia in Heavy-Ion Collisions,” *Nucl. Phys.* **A943** (2015) 147–158, arXiv:1504.00670 [hep-ph].
- [40] X. Zhao, A. Emerick, and R. Rapp, “In-Medium Quarkonia at SPS, RHIC and LHC,” *Nucl. Phys.* **A904-905** (2013) 611c–614c, arXiv:1210.6583 [hep-ph].
- [41] X. Guo, S. Shi, N. Xu, Z. Xu, and P. Zhuang, “Magnetic Field Effect on Charmonium Production in High Energy Nuclear Collisions,” *Phys. Lett.* **B751** (2015) 215–219, arXiv:1502.04407 [hep-ph].
- [42] ALICE Collaboration, B. B. Abelev *et al.*, “Elliptic flow of identified hadrons in Pb-Pb collisions at $\sqrt{s_{\text{NN}}} = 2.76$ TeV,” *JHEP* **06** (2015) 190, arXiv:1405.4632 [nucl-ex].
- [43] ALICE Collaboration, S. Acharya *et al.*, “D-meson azimuthal anisotropy in mid-central Pb-Pb collisions at $\sqrt{s_{\text{NN}}} = 5.02$ TeV,” arXiv:1707.01005 [nucl-ex].

A The ALICE Collaboration

S. Acharya¹³⁷, D. Adamová⁹⁴, J. Adolfsson³⁴, M.M. Aggarwal⁹⁹, G. Aglieri Rinella³⁵, M. Agnello³¹, N. Agrawal⁴⁸, Z. Ahammed¹³⁷, S.U. Ahn⁷⁹, S. Aiola¹⁴¹, A. Akimov⁶⁴, M. Al-Turany¹⁰⁶, S.N. Alam¹³⁷, D.S.D. Albuquerque¹²², D. Aleksandrov⁹⁰, B. Alessandro⁵⁸, R. Alfaro Molina⁷⁴, Y. Ali¹⁵, A. Alici^{27, 53, 12}, A. Alkin³, J. Alme²², T. Alt⁷⁰, L. Altenkamper²², I. Altsybeev¹³⁶, C. Alves Garcia Prado¹²¹, C. Andrei⁸⁷, D. Andreou³⁵, H.A. Andrews¹¹⁰, A. Andronic¹⁰⁶, V. Anguelov¹⁰⁴, C. Anson⁹⁷, T. Antičić¹⁰⁷, F. Antinori⁵⁶, P. Antonioli⁵³, R. Anwar¹²⁴, L. Aphecetche¹¹⁴, H. Appelshäuser⁷⁰, S. Arcelli²⁷, R. Arnaldi⁵⁸, O.W. Arnold^{105, 36}, I.C. Arsene²¹, M. Arslanok¹⁰⁴, B. Audurier¹¹⁴, A. Augustinus³⁵, R. Averbeck¹⁰⁶, M.D. Azmi¹⁷, A. Badalá⁵⁵, Y.W. Baek^{60, 78}, S. Bagnasco⁵⁸, R. Bailhache⁷⁰, R. Bala¹⁰¹, A. Baldisseri⁷⁵, M. Ball⁴⁵, R.C. Baral^{67, 88}, A.M. Barbano²⁶, R. Barbera²⁸, F. Barile³³, L. Barioglio²⁶, G.G. Barnaföldi¹⁴⁰, L.S. Barnby⁹³, V. Barret¹³¹, P. Bartalini⁷, K. Barth³⁵, E. Bartsch⁷⁰, N. Bastid¹³¹, S. Basu¹³⁹, G. Batigne¹¹⁴, B. Batyunya⁷⁷, P.C. Batzing²¹, J.L. Bazo Alba¹¹¹, I.G. Bearden⁹¹, H. Beck¹⁰⁴, C. Bedda⁶³, N.K. Behera⁶⁰, I. Belikov¹³³, F. Bellini^{27, 35}, H. Bello Martinez², R. Bellwied¹²⁴, L.G.E. Beltran¹²⁰, V. Belyaev⁸³, G. Bencedi¹⁴⁰, S. Beole²⁶, A. Bercuci⁸⁷, Y. Berdnikov⁹⁶, D. Berenyi¹⁴⁰, R.A. Bertens¹²⁷, D. Berzano³⁵, L. Betev³⁵, A. Bhasin¹⁰¹, I.R. Bhat¹⁰¹, B. Bhattacharjee⁴⁴, J. Bhom¹¹⁸, A. Bianchi²⁶, L. Bianchi¹²⁴, N. Bianchi⁵¹, C. Bianchin¹³⁹, J. Bielčák³⁹, J. Bielčiková⁹⁴, A. Bilandzic^{36, 105}, G. Biro¹⁴⁰, R. Biswas⁴, S. Biswas⁴, J.T. Blair¹¹⁹, D. Blau⁹⁰, C. Blume⁷⁰, G. Boca¹³⁴, F. Bock³⁵, A. Bogdanov⁸³, L. Boldizsár¹⁴⁰, M. Bombara⁴⁰, G. Bonomi¹³⁵, M. Bonora³⁵, J. Book⁷⁰, H. Borel⁷⁵, A. Borissov^{104, 19}, M. Borri¹²⁶, E. Botta²⁶, C. Bourjau⁹¹, L. Bratrud⁷⁰, P. Braun-Munzinger¹⁰⁶, M. Bregant¹²¹, T.A. Broker⁷⁰, M. Broz³⁹, E.J. Brucken⁴⁶, E. Bruna⁵⁸, G.E. Bruno^{35, 33}, D. Budnikov¹⁰⁸, H. Buesching⁷⁰, S. Bufalino³¹, P. Buhler¹¹³, P. Buncic³⁵, O. Busch¹³⁰, Z. Buthelezi⁷⁶, J.B. Butt¹⁵, J.T. Buxton¹⁸, J. Cabala¹¹⁶, D. Caffarri^{35, 92}, H. Caines¹⁴¹, A. Caliva^{63, 106}, E. Calvo Villar¹¹¹, P. Camerini²⁵, A.A. Capon¹¹³, F. Carena³⁵, W. Carena³⁵, F. Carnesecchi^{27, 12}, J. Castillo Castellanos⁷⁵, A.J. Castro¹²⁷, E.A.R. Casula⁵⁴, C. Ceballos Sanchez⁹, S. Chandra¹³⁷, B. Chang¹²⁵, W. Chang⁷, S. Chapeland³⁵, M. Chartier¹²⁶, S. Chattopadhyay¹³⁷, S. Chattopadhyay¹⁰⁹, A. Chauvin^{36, 105}, C. Cheshkov¹³², B. Cheynis¹³², V. Chibante Barroso³⁵, D.D. Chinellato¹²², S. Cho⁶⁰, P. Chochula³⁵, M. Chojnacki⁹¹, S. Choudhury¹³⁷, T. Chowdhury¹³¹, P. Christakoglou⁹², C.H. Christensen⁹¹, P. Christiansen³⁴, T. Chujo¹³⁰, S.U. Chung¹⁹, C. Cicalo⁵⁴, L. Cifarelli^{12, 27}, F. Cindolo⁵³, J. Cleymans¹⁰⁰, F. Colamaria^{52, 33}, D. Colella^{35, 52, 65}, A. Collu⁸², M. Colocci²⁷, M. Concas^{58, ii}, G. Conesa Balbastre⁸¹, Z. Conesa del Valle⁶¹, J.G. Contreras³⁹, T.M. Cormier⁹⁵, Y. Corrales Morales⁵⁸, I. Cortés Maldonado², P. Cortese³², M.R. Cosentino¹²³, F. Costa³⁵, S. Costanza¹³⁴, J. Crkovská⁶¹, P. Crochet¹³¹, E. Cuautele⁷², L. Cunqueiro^{95, 71}, T. Dahms^{36, 105}, A. Dainese⁵⁶, M.C. Danisch¹⁰⁴, A. Danu⁶⁸, D. Das¹⁰⁹, I. Das¹⁰⁹, S. Das⁴, A. Dash⁸⁸, S. Dash⁴⁸, S. De⁴⁹, A. De Caro³⁰, G. de Cataldo⁵², C. de Conti¹²¹, J. de Cuveland⁴², A. De Falco²⁴, D. De Gruttola^{30, 12}, N. De Marco⁵⁸, S. De Pasquale³⁰, R.D. De Souza¹²², H.F. Degenhardt¹²¹, A. Deisting^{106, 104}, A. Deloff⁸⁶, C. Deplano⁹², P. Dhankeer⁴⁸, D. Di Bari³³, A. Di Mauro³⁵, P. Di Nezza⁵¹, B. Di Ruzza⁵⁶, M.A. Diaz Corchero¹⁰, T. Dietel¹⁰⁰, P. Dillenseger⁷⁰, Y. Ding⁷, R. Diviá³⁵, Ø. Djuvland²², A. Dobrin³⁵, D. Domenicis Gimenez¹²¹, B. Dönigus⁷⁰, O. Dordic²¹, L.V.R. Doremalen⁶³, A.K. Dubey¹³⁷, A. Dubla¹⁰⁶, L. Ducroux¹³², S. Dudi⁹⁹, A.K. Duggal⁹⁹, M. Dukhishyam⁸⁸, P. Dupieux¹³¹, R.J. Ehlers¹⁴¹, D. Elia⁵², E. Endress¹¹¹, H. Engel⁶⁹, E. Epple¹⁴¹, B. Erazmus¹¹⁴, F. Erhardt⁹⁸, B. Espagnon⁶¹, G. Eulisse³⁵, J. Eum¹⁹, D. Evans¹¹⁰, S. Evdokimov¹¹², L. Fabbietti^{105, 36}, J. Faivre⁸¹, A. Fantoni⁵¹, M. Fasel⁹⁵, L. Feldkamp⁷¹, A. Feliciello⁵⁸, G. Feofilov¹³⁶, A. Fernández Téllez², E.G. Ferreira¹⁶, A. Ferretti²⁶, A. Festanti^{29, 35}, V.J.G. Feuillard^{75, 131}, J. Figiel¹¹⁸, M.A.S. Figueredo¹²¹, S. Filchagin¹⁰⁸, D. Finogeev⁶², F.M. Fionda^{22, 24}, M. Floris³⁵, S. Foertsch⁷⁶, P. Foka¹⁰⁶, S. Fokin⁹⁰, E. Fragiaco⁵⁹, A. Francescon³⁵, A. Francisco¹¹⁴, U. Frankenfeld¹⁰⁶, G.G. Fronze²⁶, U. Fuchs³⁵, C. Furget⁸¹, A. Furs⁶², M. Fusco Girard³⁰, J.J. Gaardhøje⁹¹, M. Gagliardi²⁶, A.M. Gago¹¹¹, K. Gajdosova⁹¹, M. Gallio²⁶, C.D. Galvan¹²⁰, P. Ganoti⁸⁵, C. Garabatos¹⁰⁶, E. Garcia-Solis¹³, K. Garg²⁸, C. Gargiulo³⁵, P. Gasik^{105, 36}, E.F. Gauger¹¹⁹, M.B. Gay Ducati⁷³, M. Germain¹¹⁴, J. Ghosh¹⁰⁹, P. Ghosh¹³⁷, S.K. Ghosh⁴, P. Gianotti⁵¹, P. Giubellino^{35, 106, 58}, P. Giubilato²⁹, E. Gladysz-Dziadus¹¹⁸, P. Glässer¹⁰⁴, D.M. Gómez Coral⁷⁴, A. Gomez Ramirez⁶⁹, A.S. Gonzalez³⁵, V. Gonzalez¹⁰, P. González-Zamora^{10, 2}, S. Gorbunov⁴², L. Görlich¹¹⁸, S. Gotovac¹¹⁷, V. Grabski⁷⁴, L.K. Graczykowski¹³⁸, K.L. Graham¹¹⁰, L. Greiner⁸², A. Grelli⁶³, C. Grigoras³⁵, V. Grigoriev⁸³, A. Grigoryan¹, S. Grigoryan⁷⁷, J.M. Gronefeld¹⁰⁶, F. Grosa³¹, J.F. Grosse-Oetringhaus³⁵, R. Grosso¹⁰⁶, F. Guber⁶², R. Guernane⁸¹, B. Guerzoni²⁷, K. Gulbrandsen⁹¹, T. Gunji¹²⁹, A. Gupta¹⁰¹, R. Gupta¹⁰¹, I.B. Guzman², R. Haake³⁵, C. Hadjidakis⁶¹, H. Hamagaki⁸⁴, G. Hamar¹⁴⁰, J.C. Hamon¹³³, M.R. Haque⁶³, J.W. Harris¹⁴¹, A. Harton¹³, H. Hassan⁸¹, D. Hatzifotiadou^{12, 53}, S. Hayashi¹²⁹, S.T. Heckel⁷⁰, E. Hellbär⁷⁰, H. Helstrup³⁷, A. Hergelegiu⁸⁷, E.G. Hernandez², G. Herrera Corral¹¹, F. Herrmann⁷¹, B.A. Hess¹⁰³, K.F. Hetland³⁷, H. Hillemanns³⁵, C. Hills¹²⁶, B. Hippolyte¹³³, B. Hohlweger¹⁰⁵, D. Horak³⁹, S. Hornung¹⁰⁶, R. Hosokawa^{81, 130}, P. Hristov³⁵,

C. Hughes¹²⁷, T.J. Humanic¹⁸, N. Hussain⁴⁴, T. Hussain¹⁷, D. Hutter⁴², D.S. Hwang²⁰, S.A. Iga Buitron⁷², R. Ilkaev¹⁰⁸, M. Inaba¹³⁰, M. Ippolitov^{83,90}, M.S. Islam¹⁰⁹, M. Ivanov¹⁰⁶, V. Ivanov⁹⁶, V. Izucheev¹¹², B. Jacak⁸², N. Jacazio²⁷, P.M. Jacobs⁸², M.B. Jadhav⁴⁸, S. Jadlovská¹¹⁶, J. Jadlovsky¹¹⁶, S. Jaelani⁶³, C. Jahnke³⁶, M.J. Jakubowska¹³⁸, M.A. Janik¹³⁸, P.H.S.Y. Jayarathna¹²⁴, C. Jena⁸⁸, M. Jercic⁹⁸, R.T. Jimenez Bustamante¹⁰⁶, P.G. Jones¹¹⁰, A. Jusko¹¹⁰, P. Kalinak⁶⁵, A. Kalweit³⁵, J.H. Kang¹⁴², V. Kaplin⁸³, S. Kar¹³⁷, A. Karasu Uysal⁸⁰, O. Karavichev⁶², T. Karavicheva⁶², L. Karayan^{106,104}, P. Karczmarczyk³⁵, E. Karpechev⁶², U. Kebschull⁶⁹, R. Keidel¹⁴³, D.L.D. Keijdener⁶³, M. Keil³⁵, B. Ketzer⁴⁵, Z. Khabanova⁹², P. Khan¹⁰⁹, S.A. Khan¹³⁷, A. Khanzadeev⁹⁶, Y. Kharlov¹¹², A. Khatun¹⁷, A. Khuntia⁴⁹, M.M. Kielbowicz¹¹⁸, B. Kileng³⁷, B. Kim¹³⁰, D. Kim¹⁴², D.J. Kim¹²⁵, H. Kim¹⁴², J.S. Kim⁴³, J. Kim¹⁰⁴, M. Kim⁶⁰, S. Kim²⁰, T. Kim¹⁴², S. Kirsch⁴², I. Kisel⁴², S. Kiselev⁶⁴, A. Kisiel¹³⁸, G. Kiss¹⁴⁰, J.L. Klay⁶, C. Klein⁷⁰, J. Klein³⁵, C. Klein-Bösing⁷¹, S. Klewin¹⁰⁴, A. Kluge³⁵, M.L. Knichel^{104,35}, A.G. Knospe¹²⁴, C. Kobdaj¹¹⁵, M. Kofarago¹⁴⁰, M.K. Köhler¹⁰⁴, T. Kollegger¹⁰⁶, V. Kondratiev¹³⁶, N. Kondratyeva⁸³, E. Kondratyuk¹¹², A. Konevskikh⁶², M. Konyushikhin¹³⁹, M. Kopcik¹¹⁶, M. Kour¹⁰¹, C. Kouzinopoulos³⁵, O. Kovalenko⁸⁶, V. Kovalenko¹³⁶, M. Kowalski¹¹⁸, G. Koyithatta Meethalevedu⁴⁸, I. Králik⁶⁵, A. Kravčáková⁴⁰, L. Kreis¹⁰⁶, M. Krivda^{110,65}, F. Krizek⁹⁴, E. Kryshen⁹⁶, M. Krzewicki⁴², A.M. Kubera¹⁸, V. Kučera⁹⁴, C. Kuhn¹³³, P.G. Kuijer⁹², A. Kumar¹⁰¹, J. Kumar⁴⁸, L. Kumar⁹⁹, S. Kumar⁴⁸, S. Kundu⁸⁸, P. Kurashvili⁸⁶, A. Kurepin⁶², A.B. Kurepin⁶², A. Kuryakin¹⁰⁸, S. Kuschpil⁹⁴, M.J. Kweon⁶⁰, Y. Kwon¹⁴², S.L. La Pointe⁴², P. La Rocca²⁸, C. Lagana Fernandes¹²¹, Y.S. Lai⁸², I. Lakomov³⁵, R. Langoy⁴¹, K. Lapidus¹⁴¹, C. Lara⁶⁹, A. Lardeux²¹, A. Lattuca²⁶, E. Laudi³⁵, R. Lavicka³⁹, R. Lea²⁵, L. Leardini¹⁰⁴, S. Lee¹⁴², F. Lehas⁹², S. Lehner¹¹³, J. Lehrbach⁴², R.C. Lemmon⁹³, E. Leogrande⁶³, I. León Monzón¹²⁰, P. Lévai¹⁴⁰, X. Li¹⁴, J. Lien⁴¹, R. Lietava¹¹⁰, B. Lim¹⁹, S. Lindal²¹, V. Lindenstruth⁴², S.W. Lindsay¹²⁶, C. Lippmann¹⁰⁶, M.A. Lisa¹⁸, V. Litichevskyi⁴⁶, W.J. Llope¹³⁹, D.F. Lodato⁶³, P.I. Loenne²², V. Loginov⁸³, C. Loizides^{95,82}, P. Loncar¹¹⁷, X. Lopez¹³¹, E. López Torres⁹, A. Lowe¹⁴⁰, P. Luettig⁷⁰, J.R. Luhder⁷¹, M. Lunardon²⁹, G. Luparello^{59,25}, M. Lupi³⁵, T.H. Lutz¹⁴¹, A. Maevskaya⁶², M. Mager³⁵, S.M. Mahmood²¹, A. Maire¹³³, R.D. Majka¹⁴¹, M. Malaev⁹⁶, L. Malinina^{77,iii}, D. Mal'Kevich⁶⁴, P. Malzacher¹⁰⁶, A. Mamonov¹⁰⁸, V. Manko⁹⁰, F. Manso¹³¹, V. Manzari⁵², Y. Mao⁷, M. Marchisone^{132,76,128}, J. Mareš⁶⁶, G.V. Margagliotti²⁵, A. Margotti⁵³, J. Margutti⁶³, A. Marín¹⁰⁶, C. Markert¹¹⁹, M. Marquard⁷⁰, N.A. Martin¹⁰⁶, P. Martinengo³⁵, J.A.L. Martínez⁶⁹, M.I. Martínez², G. Martínez García¹¹⁴, M. Martínez Pedreira³⁵, S. Masciocchi¹⁰⁶, M. Masea²⁶, A. Masoni⁵⁴, E. Masson¹¹⁴, A. Mastroserio⁵², A.M. Mathis^{105,36}, P.F.T. Matuoka¹²¹, A. Matyjka¹²⁷, C. Mayer¹¹⁸, J. Mazer¹²⁷, M. Mazzilli³³, M.A. Mazzoni⁵⁷, F. Meddi²³, Y. Melikyan⁸³, A. Menchaca-Rocha⁷⁴, E. Meninno³⁰, J. Mercado Pérez¹⁰⁴, M. Meres³⁸, S. Mhlanga¹⁰⁰, Y. Miake¹³⁰, M.M. Mieskolainen⁴⁶, D.L. Mihaylov¹⁰⁵, K. Mikhaylov^{64,77}, A. Mischke⁶³, A.N. Mishra⁴⁹, D. Miśkowiec¹⁰⁶, J. Mitra¹³⁷, C.M. Miti⁶⁸, N. Mohammadi⁶³, A.P. Mohanty⁶³, B. Mohanty⁸⁸, M. Mohisin Khan^{17,iv}, E. Montes¹⁰, D.A. Moreira De Godoy⁷¹, L.A.P. Moreno², S. Moretto²⁹, A. Morreale¹¹⁴, A. Morsch³⁵, V. Muccifora⁵¹, E. Mudnic¹¹⁷, D. Mühlheim⁷¹, S. Muhuri¹³⁷, M. Mukherjee⁴, J.D. Mulligan¹⁴¹, M.G. Munhoz¹²¹, K. Munning⁴⁵, R.H. Munzer⁷⁰, H. Murakami¹²⁹, S. Murray⁷⁶, L. Musa³⁵, J. Musinsky⁶⁵, C.J. Myers¹²⁴, J.W. Myrcha¹³⁸, D. Nag⁴, B. Naik⁴⁸, R. Nair⁸⁶, B.K. Nandi⁴⁸, R. Nania^{12,53}, E. Nappi⁵², A. Narayan⁴⁸, M.U. Naru¹⁵, H. Natal da Luz¹²¹, C. Natrass¹²⁷, S.R. Navarro², K. Nayak⁸⁸, R. Nayak⁴⁸, T.K. Nayak¹³⁷, S. Nazarenko¹⁰⁸, R.A. Negrao De Oliveira³⁵, L. Nellen⁷², S.V. Nesbo³⁷, F. Ng¹²⁴, M. Nicassio¹⁰⁶, M. Niculescu⁶⁸, J. Niedziela^{138,35}, B.S. Nielsen⁹¹, S. Nikolaev⁹⁰, S. Nikulin⁹⁰, V. Nikulin⁹⁶, F. Noferini^{12,53}, P. Nomokonov⁷⁷, G. Nooren⁶³, J.C.C. Noris², J. Norman¹²⁶, A. Nyman⁹⁰, J. Nystrand²², H. Oeschler^{104,19,i}, A. Ohlson¹⁰⁴, T. Okubo⁴⁷, L. Olah¹⁴⁰, J. Oleniacz¹³⁸, A.C. Oliveira Da Silva¹²¹, M.H. Oliver¹⁴¹, J. Onderwaater¹⁰⁶, C. Oppedisano⁵⁸, R. Orava⁴⁶, M. Oravec¹¹⁶, A. Ortiz Velasquez⁷², A. Oskarsson³⁴, J. Otwinowski¹¹⁸, K. Oyama⁸⁴, Y. Pachmayer¹⁰⁴, V. Pacik⁹¹, D. Pagano¹³⁵, G. Paic⁷², P. Palni⁷, J. Pan¹³⁹, A.K. Pandey⁴⁸, S. Panebianco⁷⁵, V. Papikyan¹, P. Pareek⁴⁹, J. Park⁶⁰, S. Parmar⁹⁹, A. Passfeld⁷¹, S.P. Pathak¹²⁴, R.N. Patra¹³⁷, B. Paul⁵⁸, H. Pei⁷, T. Peitzmann⁶³, X. Peng⁷, L.G. Pereira⁷³, H. Pereira Da Costa⁷⁵, D. Peresunko^{83,90}, E. Perez Lezama⁷⁰, V. Peskov⁷⁰, Y. Pestov⁵, V. Petráček³⁹, V. Petrov¹¹², M. Petrovici⁸⁷, C. Petta²⁸, R.P. Pezzi⁷³, S. Piano⁵⁹, M. Pika³⁸, P. Pillot¹¹⁴, L.O.D.L. Pimentel⁹¹, O. Pinazza^{53,35}, L. Pinsky¹²⁴, D.B. Piyarathna¹²⁴, M. Płoskoń⁸², M. Planinic⁹⁸, F. Pliquett⁷⁰, J. Pluta¹³⁸, S. Pochybova¹⁴⁰, P.L.M. Podesta-Lerma¹²⁰, M.G. Poghosyan⁹⁵, B. Polichtchouk¹¹², N. Poljak⁹⁸, W. Poonsawat¹¹⁵, A. Pop⁸⁷, H. Poppenborg⁷¹, S. Porteboeuf-Houssais¹³¹, V. Pozdniakov⁷⁷, S.K. Prasad⁴, R. Preghenella⁵³, F. Prino⁵⁸, C.A. Pruneau¹³⁹, I. Pshenichnov⁶², M. Puccio²⁶, V. Punin¹⁰⁸, J. Putschke¹³⁹, S. Raha⁴, S. Rajput¹⁰¹, J. Rak¹²⁵, A. Rakotozafindrabe⁷⁵, L. Ramello³², F. Rami¹³³, D.B. Rana¹²⁴, R. Raniwala¹⁰², S. Raniwala¹⁰², S.S. Räsänen⁴⁶, B.T. Rascanu⁷⁰, D. Rathee⁹⁹, V. Ratza⁴⁵, I. Ravasenga³¹, K.F. Read^{127,95}, K. Redlich^{86,v}, A. Rehman²², P. Reichelt⁷⁰, F. Reidt³⁵, X. Ren⁷, R. Renfordt⁷⁰, A. Reshetin⁶², K. Reygers¹⁰⁴, V. Riabov⁹⁶, T. Richert^{63,34}, M. Richter²¹, P. Riedler³⁵,

W. Riegler³⁵, F. Riggi²⁸, C. Ristea⁶⁸, M. Rodríguez Cahuantzi², K. Røed²¹, E. Rogochaya⁷⁷, D. Rohr^{35,42}, D. Röhrich²², P.S. Rokita¹³⁸, F. Ronchetti⁵¹, E.D. Rosas⁷², P. Rosnet¹³¹, A. Rossi^{29,56}, A. Rotondi¹³⁴, F. Roukoutakis⁸⁵, C. Roy¹³³, P. Roy¹⁰⁹, A.J. Rubio Montero¹⁰, O.V. Rueda⁷², R. Rui²⁵, B. Rumyantsev⁷⁷, A. Rustamov⁸⁹, E. Ryabinkin⁹⁰, Y. Ryabov⁹⁶, A. Rybicki¹¹⁸, S. Saarinen⁴⁶, S. Sadhu¹³⁷, S. Sadovsky¹¹², K. Šafařík³⁵, S.K. Saha¹³⁷, B. Sahlmuller⁷⁰, B. Sahoo⁴⁸, P. Sahoo⁴⁹, R. Sahoo⁴⁹, S. Sahoo⁶⁷, P.K. Sahu⁶⁷, J. Saini¹³⁷, S. Sakai¹³⁰, M.A. Saleh¹³⁹, J. Salzwedel¹⁸, S. Sambyal¹⁰¹, V. Samsonov^{96,83}, A. Sandoval⁷⁴, A. Sarkar⁷⁶, D. Sarkar¹³⁷, N. Sarkar¹³⁷, P. Sarma⁴⁴, M.H.P. Sas⁶³, E. Scapparone⁵³, F. Scarlassara²⁹, B. Schaefer⁹⁵, H.S. Scheid⁷⁰, C. Schiaua⁸⁷, R. Schicker¹⁰⁴, C. Schmidt¹⁰⁶, H.R. Schmidt¹⁰³, M.O. Schmidt¹⁰⁴, M. Schmidt¹⁰³, N.V. Schmidt^{70,95}, J. Schukraft³⁵, Y. Schutz^{35,133}, K. Schwarz¹⁰⁶, K. Schweda¹⁰⁶, G. Scioli²⁷, E. Scomparin⁵⁸, M. Šefčík⁴⁰, J.E. Seger⁹⁷, Y. Sekiguchi¹²⁹, D. Sekihata⁴⁷, I. Selyuzhenkov^{106,83}, K. Senosi⁷⁶, S. Senyukov¹³³, E. Serradilla^{10,74}, P. Sett⁴⁸, A. Sevcenco⁶⁸, A. Shabanov⁶², A. Shabetai¹¹⁴, R. Shahoyan³⁵, W. Shaikh¹⁰⁹, A. Shangaraev¹¹², A. Sharma⁹⁹, A. Sharma¹⁰¹, M. Sharma¹⁰¹, M. Sharma¹⁰¹, N. Sharma⁹⁹, A.I. Sheikh¹³⁷, K. Shigaki⁴⁷, S. Shirinkin⁶⁴, Q. Shou⁷, K. Shtejer^{9,26}, Y. Sibiriak⁹⁰, S. Siddhanta⁵⁴, K.M. Sielewicz³⁵, T. Siemiarczuk⁸⁶, S. Silaeva⁹⁰, D. Silvermyr³⁴, G. Simatovic⁹², G. Simonetti³⁵, R. Singaraju¹³⁷, R. Singh⁸⁸, V. Singhal¹³⁷, T. Sinha¹⁰⁹, B. Sitar³⁸, M. Sitta³², T.B. Skaali²¹, M. Slupecki¹²⁵, N. Smirnov¹⁴¹, R.J.M. Snellings⁶³, T.W. Snellman¹²⁵, J. Song¹⁹, M. Song¹⁴², F. Soramel²⁹, S. Sorensen¹²⁷, F. Sozzi¹⁰⁶, I. Sputowska¹¹⁸, J. Stachel¹⁰⁴, I. Stan⁶⁸, P. Stankus⁹⁵, E. Stenlund³⁴, D. Stocco¹¹⁴, M.M. Storetvedt³⁷, P. Strmen³⁸, A.A.P. Suaide¹²¹, T. Sugitate⁴⁷, C. Suire⁶¹, M. Suleymanov¹⁵, M. Suljic²⁵, R. Sultanov⁶⁴, M. Šumbera⁹⁴, S. Sumowidagdo⁵⁰, K. Suzuki¹¹³, S. Swain⁶⁷, A. Szabo³⁸, I. Szarka³⁸, U. Tabassam¹⁵, J. Takahashi¹²², G.J. Tambave²², N. Tanaka¹³⁰, M. Tarhini⁶¹, M. Tariq¹⁷, M.G. Tarzila⁸⁷, A. Tauro³⁵, G. Tejeda Muñoz², A. Telesca³⁵, K. Terasaki¹²⁹, C. Terrevoli²⁹, B. Teyssier¹³², D. Thakur⁴⁹, S. Thakur¹³⁷, D. Thomas¹¹⁹, F. Thoresen⁹¹, R. Tieulent¹³², A. Tikhonov⁶², A.R. Timmins¹²⁴, A. Toia⁷⁰, M. Toppi⁵¹, S.R. Torres¹²⁰, S. Tripathy⁴⁹, S. Trogolo²⁶, G. Trombetta³³, L. Tropp⁴⁰, V. Trubnikov³, W.H. Trzaska¹²⁵, B.A. Trzeciak⁶³, T. Tsuji¹²⁹, A. Tumkin¹⁰⁸, R. Turrisi⁵⁶, T.S. Tveter²¹, K. Ullaland²², E.N. Umaka¹²⁴, A. Uras¹³², G.L. Usai²⁴, A. Utrobicic⁹⁸, M. Vala^{116,65}, J. Van Der Maarel⁶³, J.W. Van Hoorne³⁵, M. van Leeuwen⁶³, T. Vanat⁹⁴, P. Vande Vyvre³⁵, D. Varga¹⁴⁰, A. Vargas², M. Vargyas¹²⁵, R. Varma⁴⁸, M. Vasileiou⁸⁵, A. Vasiliev⁹⁰, A. Vauthier⁸¹, O. Vázquez Doce^{105,36}, V. Vechernin¹³⁶, A.M. Veen⁶³, A. Velure²², E. Vercellin²⁶, S. Vergara Limón², R. Vernet⁸, R. Vértesi¹⁴⁰, L. Vickovic¹¹⁷, S. Vigolo⁶³, J. Viinikainen¹²⁵, Z. Vilakazi¹²⁸, O. Villalobos Baillie¹¹⁰, A. Villatoro Tello², A. Vinogradov⁹⁰, L. Vinogradov¹³⁶, T. Virgili³⁰, V. Vislavicius³⁴, A. Vodopyanov⁷⁷, M.A. Völkl¹⁰³, K. Voloshin⁶⁴, S.A. Voloshin¹³⁹, G. Volpe³³, B. von Haller³⁵, I. Vorobyev^{105,36}, D. Voscek¹¹⁶, D. Vranic^{35,106}, J. Vrláková⁴⁰, B. Wagner²², H. Wang⁶³, M. Wang⁷, D. Watanabe¹³⁰, Y. Watanabe^{129,130}, M. Weber¹¹³, S.G. Weber¹⁰⁶, D.F. Weiser¹⁰⁴, S.C. Wenzel³⁵, J.P. Wessels⁷¹, U. Westerhoff⁷¹, A.M. Whitehead¹⁰⁰, J. Wiechula⁷⁰, J. Wikne²¹, G. Wilk⁸⁶, J. Wilkinson^{104,53}, G.A. Willems^{35,71}, M.C.S. Williams⁵³, E. Willsher¹¹⁰, B. Windelband¹⁰⁴, W.E. Witt¹²⁷, R. Xu⁷, S. Yalcin⁸⁰, K. Yamakawa⁴⁷, P. Yang⁷, S. Yano⁴⁷, Z. Yin⁷, H. Yokoyama^{130,81}, I.-K. Yoo¹⁹, J.H. Yoon⁶⁰, E. Yun¹⁹, V. Yurchenko³, V. Zaccolo⁵⁸, A. Zaman¹⁵, C. Zampolli³⁵, H.J.C. Zanolli¹²¹, N. Zardoshti¹¹⁰, A. Zarochentsev¹³⁶, P. Závada⁶⁶, N. Zaviyalov¹⁰⁸, H. Zbroszczyk¹³⁸, M. Zhalov⁹⁶, H. Zhang^{22,7}, X. Zhang⁷, Y. Zhang⁷, C. Zhang⁶³, Z. Zhang^{7,131}, C. Zhao²¹, N. Zhigareva⁶⁴, D. Zhou⁷, Y. Zhou⁹¹, Z. Zhou²², H. Zhu²², J. Zhu⁷, Y. Zhu⁷, A. Zichichi^{12,27}, M.B. Zimmermann³⁵, G. Zinovjev³, J. Zmeskal¹¹³, S. Zou⁷,

Affiliation notes

ⁱ Deceased

ⁱⁱ Dipartimento DET del Politecnico di Torino, Turin, Italy

ⁱⁱⁱ M.V. Lomonosov Moscow State University, D.V. Skobeltsyn Institute of Nuclear Physics, Moscow, Russia

^{iv} Department of Applied Physics, Aligarh Muslim University, Aligarh, India

^v Institute of Theoretical Physics, University of Wrocław, Poland

Collaboration Institutes

¹ A.I. Alikhanyan National Science Laboratory (Yerevan Physics Institute) Foundation, Yerevan, Armenia

² Benemérita Universidad Autónoma de Puebla, Puebla, Mexico

³ Bogolyubov Institute for Theoretical Physics, Kiev, Ukraine

⁴ Bose Institute, Department of Physics and Centre for Astroparticle Physics and Space Science (CAPSS), Kolkata, India

⁵ Budker Institute for Nuclear Physics, Novosibirsk, Russia

- 6 California Polytechnic State University, San Luis Obispo, California, United States
- 7 Central China Normal University, Wuhan, China
- 8 Centre de Calcul de l'IN2P3, Villeurbanne, Lyon, France
- 9 Centro de Aplicaciones Tecnológicas y Desarrollo Nuclear (CEADEN), Havana, Cuba
- 10 Centro de Investigaciones Energéticas Medioambientales y Tecnológicas (CIEMAT), Madrid, Spain
- 11 Centro de Investigación y de Estudios Avanzados (CINVESTAV), Mexico City and Mérida, Mexico
- 12 Centro Fermi - Museo Storico della Fisica e Centro Studi e Ricerche "Enrico Fermi", Rome, Italy
- 13 Chicago State University, Chicago, Illinois, United States
- 14 China Institute of Atomic Energy, Beijing, China
- 15 COMSATS Institute of Information Technology (CIIT), Islamabad, Pakistan
- 16 Departamento de Física de Partículas and IGFAE, Universidad de Santiago de Compostela, Santiago de Compostela, Spain
- 17 Department of Physics, Aligarh Muslim University, Aligarh, India
- 18 Department of Physics, Ohio State University, Columbus, Ohio, United States
- 19 Department of Physics, Pusan National University, Pusan, Republic of Korea
- 20 Department of Physics, Sejong University, Seoul, Republic of Korea
- 21 Department of Physics, University of Oslo, Oslo, Norway
- 22 Department of Physics and Technology, University of Bergen, Bergen, Norway
- 23 Dipartimento di Fisica dell'Università 'La Sapienza' and Sezione INFN, Rome, Italy
- 24 Dipartimento di Fisica dell'Università and Sezione INFN, Cagliari, Italy
- 25 Dipartimento di Fisica dell'Università and Sezione INFN, Trieste, Italy
- 26 Dipartimento di Fisica dell'Università and Sezione INFN, Turin, Italy
- 27 Dipartimento di Fisica e Astronomia dell'Università and Sezione INFN, Bologna, Italy
- 28 Dipartimento di Fisica e Astronomia dell'Università and Sezione INFN, Catania, Italy
- 29 Dipartimento di Fisica e Astronomia dell'Università and Sezione INFN, Padova, Italy
- 30 Dipartimento di Fisica 'E.R. Caianiello' dell'Università and Gruppo Collegato INFN, Salerno, Italy
- 31 Dipartimento DISAT del Politecnico and Sezione INFN, Turin, Italy
- 32 Dipartimento di Scienze e Innovazione Tecnologica dell'Università del Piemonte Orientale and INFN Sezione di Torino, Alessandria, Italy
- 33 Dipartimento Interateneo di Fisica 'M. Merlin' and Sezione INFN, Bari, Italy
- 34 Division of Experimental High Energy Physics, University of Lund, Lund, Sweden
- 35 European Organization for Nuclear Research (CERN), Geneva, Switzerland
- 36 Excellence Cluster Universe, Technische Universität München, Munich, Germany
- 37 Faculty of Engineering, Bergen University College, Bergen, Norway
- 38 Faculty of Mathematics, Physics and Informatics, Comenius University, Bratislava, Slovakia
- 39 Faculty of Nuclear Sciences and Physical Engineering, Czech Technical University in Prague, Prague, Czech Republic
- 40 Faculty of Science, P.J. Šafárik University, Košice, Slovakia
- 41 Faculty of Technology, Buskerud and Vestfold University College, Tonsberg, Norway
- 42 Frankfurt Institute for Advanced Studies, Johann Wolfgang Goethe-Universität Frankfurt, Frankfurt, Germany
- 43 Gangneung-Wonju National University, Gangneung, Republic of Korea
- 44 Gauhati University, Department of Physics, Guwahati, India
- 45 Helmholtz-Institut für Strahlen- und Kernphysik, Rheinische Friedrich-Wilhelms-Universität Bonn, Bonn, Germany
- 46 Helsinki Institute of Physics (HIP), Helsinki, Finland
- 47 Hiroshima University, Hiroshima, Japan
- 48 Indian Institute of Technology Bombay (IIT), Mumbai, India
- 49 Indian Institute of Technology Indore, Indore, India
- 50 Indonesian Institute of Sciences, Jakarta, Indonesia
- 51 INFN, Laboratori Nazionali di Frascati, Frascati, Italy
- 52 INFN, Sezione di Bari, Bari, Italy
- 53 INFN, Sezione di Bologna, Bologna, Italy
- 54 INFN, Sezione di Cagliari, Cagliari, Italy
- 55 INFN, Sezione di Catania, Catania, Italy
- 56 INFN, Sezione di Padova, Padova, Italy

- 57 INFN, Sezione di Roma, Rome, Italy
58 INFN, Sezione di Torino, Turin, Italy
59 INFN, Sezione di Trieste, Trieste, Italy
60 Inha University, Incheon, Republic of Korea
61 Institut de Physique Nucléaire d'Orsay (IPNO), Université Paris-Sud, CNRS-IN2P3, Orsay, France
62 Institute for Nuclear Research, Academy of Sciences, Moscow, Russia
63 Institute for Subatomic Physics of Utrecht University, Utrecht, Netherlands
64 Institute for Theoretical and Experimental Physics, Moscow, Russia
65 Institute of Experimental Physics, Slovak Academy of Sciences, Košice, Slovakia
66 Institute of Physics, Academy of Sciences of the Czech Republic, Prague, Czech Republic
67 Institute of Physics, Bhubaneswar, India
68 Institute of Space Science (ISS), Bucharest, Romania
69 Institut für Informatik, Johann Wolfgang Goethe-Universität Frankfurt, Frankfurt, Germany
70 Institut für Kernphysik, Johann Wolfgang Goethe-Universität Frankfurt, Frankfurt, Germany
71 Institut für Kernphysik, Westfälische Wilhelms-Universität Münster, Münster, Germany
72 Instituto de Ciencias Nucleares, Universidad Nacional Autónoma de México, Mexico City, Mexico
73 Instituto de Física, Universidade Federal do Rio Grande do Sul (UFRGS), Porto Alegre, Brazil
74 Instituto de Física, Universidad Nacional Autónoma de México, Mexico City, Mexico
75 IRFU, CEA, Université Paris-Saclay, Saclay, France
76 iThemba LABS, National Research Foundation, Somerset West, South Africa
77 Joint Institute for Nuclear Research (JINR), Dubna, Russia
78 Konkuk University, Seoul, Republic of Korea
79 Korea Institute of Science and Technology Information, Daejeon, Republic of Korea
80 KTO Karatay University, Konya, Turkey
81 Laboratoire de Physique Subatomique et de Cosmologie, Université Grenoble-Alpes, CNRS-IN2P3, Grenoble, France
82 Lawrence Berkeley National Laboratory, Berkeley, California, United States
83 Moscow Engineering Physics Institute, Moscow, Russia
84 Nagasaki Institute of Applied Science, Nagasaki, Japan
85 National and Kapodistrian University of Athens, Physics Department, Athens, Greece
86 National Centre for Nuclear Studies, Warsaw, Poland
87 National Institute for Physics and Nuclear Engineering, Bucharest, Romania
88 National Institute of Science Education and Research, HBNI, Jatni, India
89 National Nuclear Research Center, Baku, Azerbaijan
90 National Research Centre Kurchatov Institute, Moscow, Russia
91 Niels Bohr Institute, University of Copenhagen, Copenhagen, Denmark
92 Nikhef, Nationaal instituut voor subatomaire fysica, Amsterdam, Netherlands
93 Nuclear Physics Group, STFC Daresbury Laboratory, Daresbury, United Kingdom
94 Nuclear Physics Institute, Academy of Sciences of the Czech Republic, Řež u Prahy, Czech Republic
95 Oak Ridge National Laboratory, Oak Ridge, Tennessee, United States
96 Petersburg Nuclear Physics Institute, Gatchina, Russia
97 Physics Department, Creighton University, Omaha, Nebraska, United States
98 Physics department, Faculty of science, University of Zagreb, Zagreb, Croatia
99 Physics Department, Panjab University, Chandigarh, India
100 Physics Department, University of Cape Town, Cape Town, South Africa
101 Physics Department, University of Jammu, Jammu, India
102 Physics Department, University of Rajasthan, Jaipur, India
103 Physikalisches Institut, Eberhard Karls Universität Tübingen, Tübingen, Germany
104 Physikalisches Institut, Ruprecht-Karls-Universität Heidelberg, Heidelberg, Germany
105 Physik Department, Technische Universität München, Munich, Germany
106 Research Division and ExtreMe Matter Institute EMMI, GSI Helmholtzzentrum für Schwerionenforschung GmbH, Darmstadt, Germany
107 Rudjer Bošković Institute, Zagreb, Croatia
108 Russian Federal Nuclear Center (VNIIEF), Sarov, Russia
109 Saha Institute of Nuclear Physics, Kolkata, India
110 School of Physics and Astronomy, University of Birmingham, Birmingham, United Kingdom

- 111 Sección Física, Departamento de Ciencias, Pontificia Universidad Católica del Perú, Lima, Peru
- 112 SSC IHEP of NRC Kurchatov institute, Protvino, Russia
- 113 Stefan Meyer Institut für Subatomare Physik (SMI), Vienna, Austria
- 114 SUBATECH, IMT Atlantique, Université de Nantes, CNRS-IN2P3, Nantes, France
- 115 Suranaree University of Technology, Nakhon Ratchasima, Thailand
- 116 Technical University of Košice, Košice, Slovakia
- 117 Technical University of Split FESB, Split, Croatia
- 118 The Henryk Niewodniczanski Institute of Nuclear Physics, Polish Academy of Sciences, Cracow, Poland
- 119 The University of Texas at Austin, Physics Department, Austin, Texas, United States
- 120 Universidad Autónoma de Sinaloa, Culiacán, Mexico
- 121 Universidade de São Paulo (USP), São Paulo, Brazil
- 122 Universidade Estadual de Campinas (UNICAMP), Campinas, Brazil
- 123 Universidade Federal do ABC, Santo Andre, Brazil
- 124 University of Houston, Houston, Texas, United States
- 125 University of Jyväskylä, Jyväskylä, Finland
- 126 University of Liverpool, Liverpool, United Kingdom
- 127 University of Tennessee, Knoxville, Tennessee, United States
- 128 University of the Witwatersrand, Johannesburg, South Africa
- 129 University of Tokyo, Tokyo, Japan
- 130 University of Tsukuba, Tsukuba, Japan
- 131 Université Clermont Auvergne, CNRS/IN2P3, LPC, Clermont-Ferrand, France
- 132 Université de Lyon, Université Lyon 1, CNRS/IN2P3, IPN-Lyon, Villeurbanne, Lyon, France
- 133 Université de Strasbourg, CNRS, IPHC UMR 7178, F-67000 Strasbourg, France, Strasbourg, France
- 134 Università degli Studi di Pavia, Pavia, Italy
- 135 Università di Brescia, Brescia, Italy
- 136 V. Fock Institute for Physics, St. Petersburg State University, St. Petersburg, Russia
- 137 Variable Energy Cyclotron Centre, Kolkata, India
- 138 Warsaw University of Technology, Warsaw, Poland
- 139 Wayne State University, Detroit, Michigan, United States
- 140 Wigner Research Centre for Physics, Hungarian Academy of Sciences, Budapest, Hungary
- 141 Yale University, New Haven, Connecticut, United States
- 142 Yonsei University, Seoul, Republic of Korea
- 143 Zentrum für Technologietransfer und Telekommunikation (ZTT), Fachhochschule Worms, Worms, Germany